AFDEX
Adviser for metal Forming process Design EXpert
Newsletter
Q1 / 2024

MFRC
Metal Forming Research Corporation
www.afdex.com, mfrc@afdex.com
Tel: +82-55-755-7529, Fax: +82-55-761-7529

Contents

1. Features in AFDEX_V23R01, V23R02

AFDEX_V23R01 and V23R02 were released in 2023 April and November, respectively. Each update was introduced in the newsletter 2023 Q2 and Q3. In this newsletter, the topic lists upcoming updates and features that are planned to be included in the next release.

1.1 Shape Rolling Process Controls in Pre-processor

Previously, the basic input setting of the analysis condition is completed through the pre-processor of AFDEX, while the other inputs for specific conditions of the shape rolling process simulation such as the boundary conditions of rolls and materials were done by text file. For the convenience of use, AFDEX_V23R02 provides that all input data can be written in the pre-processor.

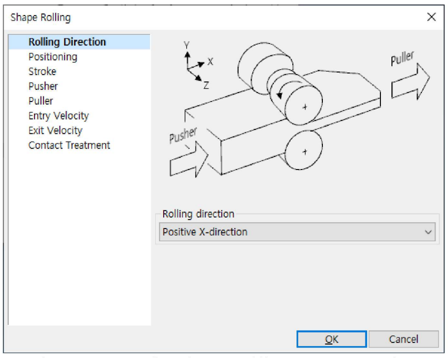

Figure 1.1 UI for shape rolling process option

1.2 Automatic Simulation of Pilgering Process

Pilger rolling process is one of incremental forming processes and a special metal forming process that combines the technology of rolling, extrusion, upsetting, etc. Pilgering process enables to mass-produce pipes with automation and eco-friendly high yield.

Recently, AFDEX provides the fully automatic simulation of the pilgering processes covering both single and composite materials. The fully automatic simulation is available using either rigid-plastic FEM or implicit elastoplastic FEM by entering the inputs involving feed rate, rotation angle, etc. A special mesh system with layers in the thickness direction is available.

Figure 1.2 shows the analysis results of the example from a reference. The simulation was fully-automatically conducted [25].

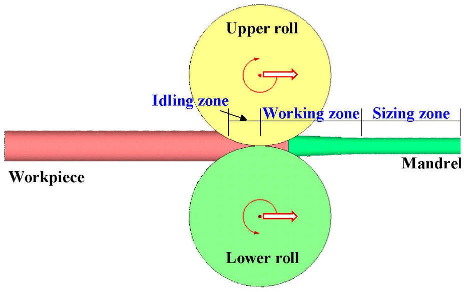

(a) Process definition

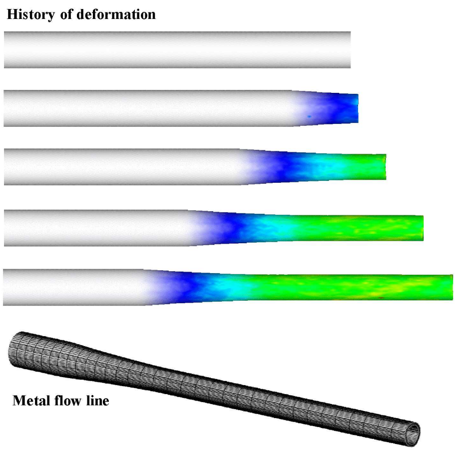

(b) Deformation, effective strain and metal flow
Figure 1.2 Simulation of pilgering process

1.3 Cone Type Roll Piercing Simulation

Barrel type roll piercing process simulation has been supported by older versions of AFDEX (M. S. Joun et al., 2014, Quantitative study on Mannesmann effect in roll piercing of hollow shaft, Procedia Engineering, Vol.81, pp.197-202). AFDEX_V23R02 provides not only the simulation of barrel type roll piercing process, but also cone type roll piercing process simulation which is used for manufacturing seamless pipes. Figure 2.2 shows a typical analysis results of cone-type roll piercing process.

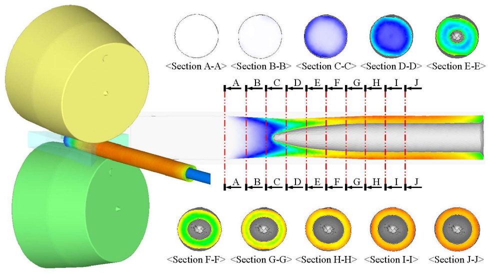

Figure 1.3 Analysis result of cone type roll piercing process

1.4 Simulation Results Compression

During the simulation, the result file may become larger in size if the number of elements or steps stored is large. In order to solve this issue, AFDEX_V23R02 provides the selective save feature which lets users save the result data of desired solution steps. Various options to select the solution steps to be newly saved are prepared. Figure 1.4 shows the UI for the selective save feature.

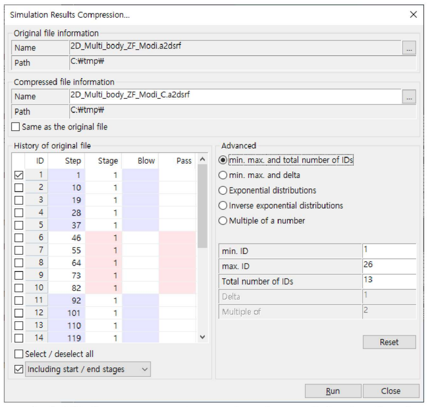

Figure 1.4 UI for supporting selection of desired solution steps to be newly saved

1.5 Scale a Workpiece Model after Forming

Since hot forging product is formed with a heated material, thermal expansion is an important consideration for the process design. The material in the state where the current analysis has been completed is one that has been subjected to thermal expansion. In the previous version, it was not possible to check the shrinkage dimensional information of the material due to cooling after forming in the post-processor. AFDEX_V23R02 provides the checking feature for the size of the material that has been shrunk using the scale adjustment function through the post-processor. Figure 1.5 shows the scale tool in pre-processor.

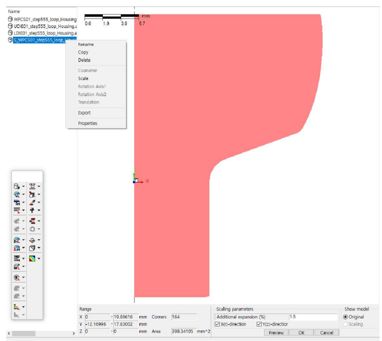

Figure 1.5 Scaling CAD model in pre-processor

1.6 UI for Inputting Translation Distance of Dies in Multi-stage Process Analysis

Multi-stage process analysis starts automatically after initializing the position of dies. In the previous version, relative position between dies inputted cannot be modified during the initialization step if two or more dies for each upper and lower dies are used for a simulation. Since this, it requires to determine accurately the relative position of dies in advance for the automatic continuous process simulation.

For most problems, this procedure is simple, while for special processes, the relative position itself is a process design factor that must be considered during process design.

In AFDEX_V23R02, the feature of changing the relative position of a die during the automatic simulation is added. For the selected die, the displacement of the rigid body movement is entered before the start of the forging stage (Figure 1.6).

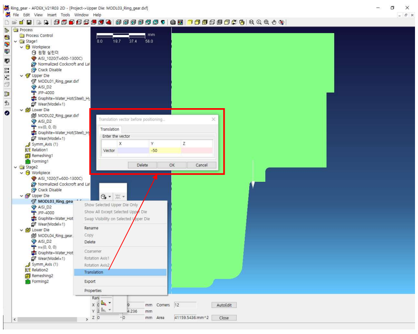

Figure 1.6 Inputs for translation distance of dies

1.7 Selective Remeshing Feature in Multi-body Simulation

Previously, remeshing had been applied to whole objects or materials during finite element analyses of multi-body structures or metal forming processes. Now, AFDEX_V23R02 provides the feature of automatic mesh density control which can find a core of a die. AFDEX_V23R02 enables users to set a remeshing feature for each object as shown in Figure 1.7. This feature can reduce the calculation time and improve the accuracy of the solution by selectively remeshing parts in the multi-body analysis.

However, if it is necessary to use the remeshing due to the extreme distortion (Negative Jacobian) on finite elements during calculation, the remeshing is performed for the entire model.

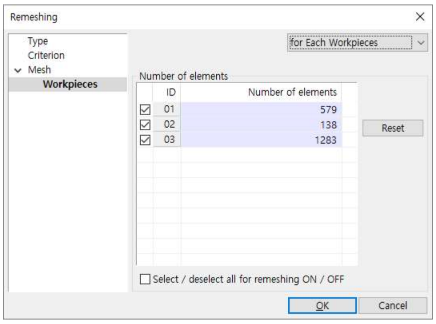

Figure 1.7 Selective remeshing option dialog box

1.8 Multilingual Support

AFDEX_V23R02 supports multilingual data and data-saving system for names of analysis input and result files, and words, phrases, and sentences in the analysis input file. Therefore, miscellaneous files are read and saved in UTF-8 format.

Also, the new version of AFDEX supports all the multilingual characters for all types of file paths, file name, and DB files. Figure 1.8 shows Japanese support on AFDEX_V23R02.

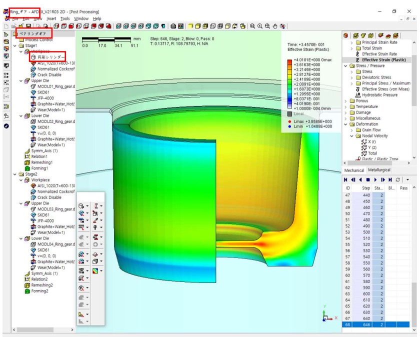

Figure 1.8 Multilingual support

1.9 Effect of Mesh Density Visualization and Density Distribution on Analysis Results

In AFDEX_SP_V23R02, 3D internal element visualization feature (Figure 1.9) and element density distribution visualization feature (Figure 1.10) are officially provided.

Figure 1.9 shows that the two meshes do not generate large errors in terms of the deformation shape of the material. Therefore, non-uniform meshes (Figure 1.9 (b)) has been recommended for the case of simulation focusing on forging possibilities in terms of computational efficiency. From an empirical point of view, however, a severe non-uniform mesh may have a negative effect on the accuracy of a result if the target is stress distribution of dies with a large local deformation. For a detailed information on this, please refer to our academic references.

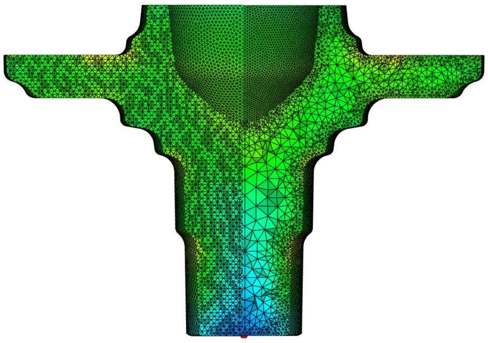

(a) Uniform mesh (b) Non-uniform (Internal coarse)

Figure 1.9 Visualization of internal mesh

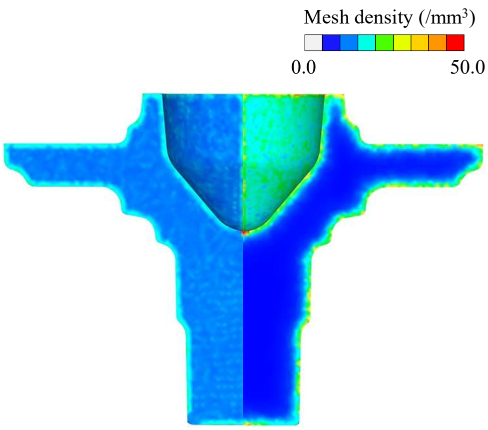

(a) Uniform mesh (b) Non-uniform (Internal coarse)

Figure 1.10 Mesh density

1.10 Number of Nodes/Elements vs. Time Plot for Multi-body Cases of Materials and Dies

AFDEX_V23R02 includes the plot with a legend for the number of nodes and elements for each die used for multi-body analysis. AFDEX_V21 and earlier versions had not provided this feature. (Figure 1.11).

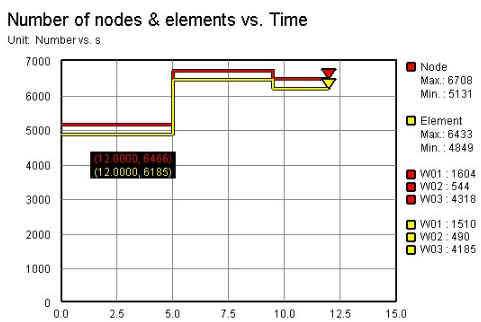

Figure 1.11 Improved UI for node/element information in multi-body analysis case

1.11 UI for Inputting Number of Elements for Remeshing in Die Structural Analysis

The mesh generation of dies is required for a die structural analysis, and high-density fine mesh can be used on a specific portion of dies. Generally, automatic mesh density control technique is applied on the die surface which is in contact with a workpiece, but user intervention can be necessary in case of special processes. Previously, input box for the number of elements of dies was included in the modeling dialog box, which was confusing for users to find it.

AFDEX_V23R02 allows users to input data of a material or a value of the number of elements for each die in the remeshing dialog box as shown in Figure 1.12.

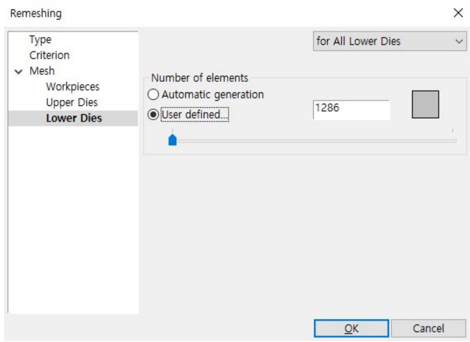

Figure 1.12 Dialog box for controlling number of elements

1.12 Improvement in Pre-processor for Crack Analysis

Recently, crack analysis conditions suitable for 2D and 3D analysis and its solvers have been improved. Due to the change in the solvers, UI of pre-processor is also updated. The criteria for element removal in 2D and 3D crack analysis are as follows:

2D: $w_1 D + w_2 \frac{\sigma_1}{\bar{\sigma}} + w_3 \frac{D\sigma_1}{\bar{\sigma}} + w_5 \frac{\dot{\bar{\varepsilon}}}{\dot{\bar{\varepsilon}}_{max}} > D_{cr}$

3D: $D > D_{cr}$ & $\dot{\bar{\varepsilon}} > \dot{\bar{\varepsilon}}_{cr}$ & $\dot{\bar{\varepsilon}} > w_5 \dot{\bar{\varepsilon}}_{max}$

where D: damage,
D_{cr}: critical damage,
w_i: weight,
$\bar{\sigma}$: yield stress,
σ_1: maximum principal stress,
$\dot{\bar{\varepsilon}}$: effective strain rate,
$\dot{\bar{\varepsilon}}_{max}$: Maximum effective strain rate.

Figure 1.13 shows new input dialog of crack analysis.

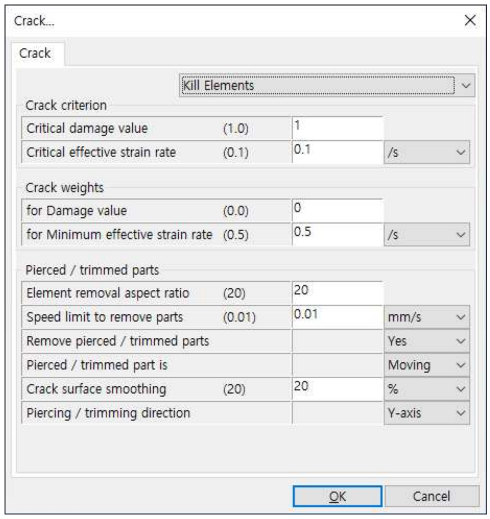

Figure 1.13 New dialog box for controlling crack simulation

1.13 Binder Feature in Plate Forging Analysis

Plate forging often uses binder which applies a blank holding force. Recently, the binder feature, which requires for unloading, has been greatly enhanced from AFDEX_V21R03 to AFDEX_V23R01 beta version. However, when a workpiece undergoes severe plastic deformation, malfunction of a binder or penetration of a material into the binder have been found and improvements in these problems are currently being made.

Figure 1.14 shows an error that occurs when the maximum compression distance of the binder is reached, and a remedy for abnormal penetration of the material into the die. Before the improvement, the material penetrated while the contact condition between the material and the binder is satisfied after the improvement.

Figure 1.15 is an example of the other error that the material rises while sticking on an upper die (Figure 1.15(a)), which is currently fixed by improving the nodal separation condition (Figure 1.15(b)).

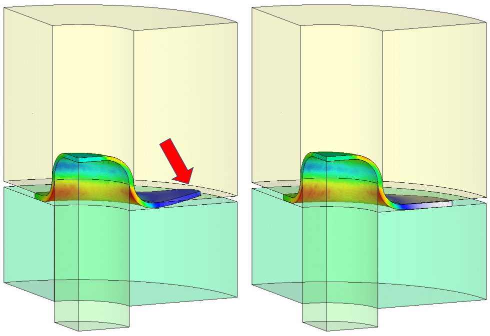

(a) Before improvement (b) After improvement
Figure 1.14 Improved binder feature

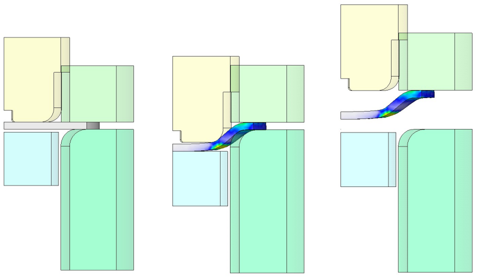

(a) Before improvement

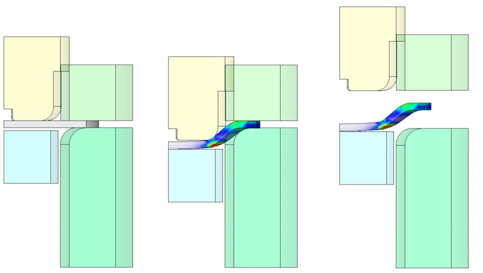

(b) After improvement
Figure 1.15 Improvement of binder feature during unloading

1.14 Reduced Load Time for Opening STL File

In the case of a large STL files or a large input file during Stage-by-stage continuous analysis, the loading of the pre-processor takes long. In the new version, the loading time of the large STL file had been dramatically reduced. For example, the loading time of about 1GB STL file shown in Figure 1.16 was reduced from 110sec to 30sec.

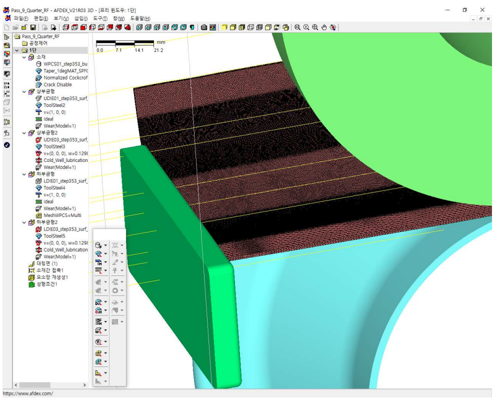

Figure 1.16 Loading a large STL file

1.15 Load-Displacement Graph View Feature

Previously, a displacement of die in load-displacement curve has been defined as the sum of maximum relative distance of die obtained in each step. It has been difficult for users to estimate the displacement when running the simulation using a binder with unknown velocity.

In new version, the maximum value among the distances of each die moved except binders will be used as a displacement in the Load-Displacement.

Figure 1.17 is an example using a die with a spring attached to Upper Die-2. In older versions, time and displacement (the absolute value of maximum velocity is 1mm/s) did not match due to the relative displacement of binder. In AFDEX_V23R02, the values of time and displacement are the same as shown in Figure 1.17.

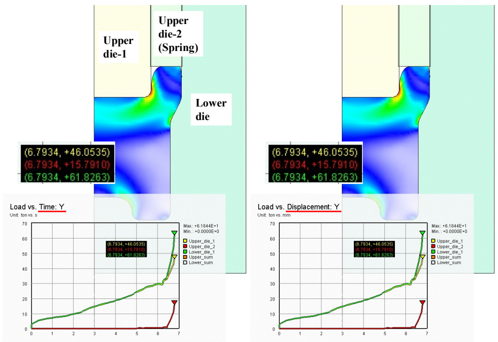

(a) Load vs. Time (b) Load vs. Displacement
Figure 1.17 Load vs. Time and Displacement plot

1.16 Feature Enhancement: Workpiece Transformation (Rotation and Translation)

Previously, two types (Vector, Table) of workpiece rotation and translation features had been supported. For 'Table' type, cases where the central axis of a workpiece was slightly misaligned occurred intermittently, when combining translation and rotation of the workpiece. To resolve this error, the 'Table' type function is improved. Also, the 'Vector' type which has been already supported can be implemented as a 'Table' type. (See Figure 1.18) In addition, the features for rotating/translating workpieces based on absolute coordinates will be provided in AFDEX V24R01.

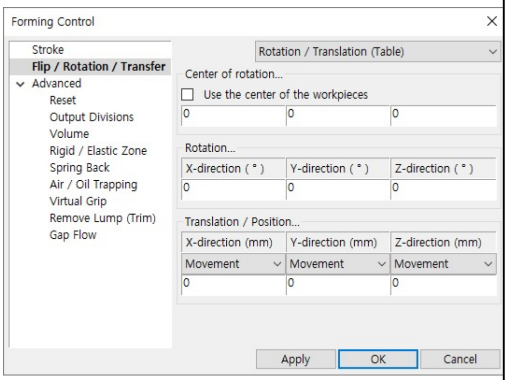

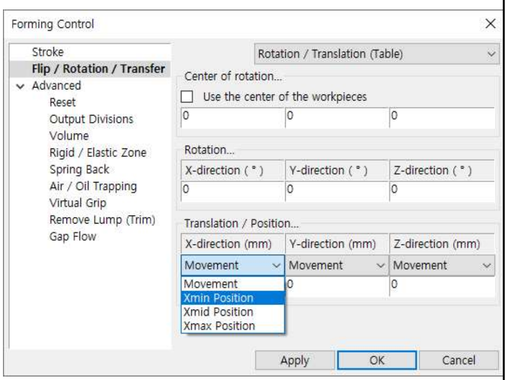

Figure 1.18 Workpiece rotation and translation

2. Upcoming Updates in AFDEX_V24R01

AFDEX_V24R01 is planned to be released on this June. The 2nd and 3rd sections list new AFDEX features, as well as other enhancements.

2.1 Pre-processor for Roll Forging Process Simulation

Up to version V23R02, there was inconvenience in using the roll forging process simulation, which ones have to apply basic conditions and boundary conditions of rolls and workpieces on the AFDEX pre-processor and *.txt file separately. As shown in Figure 2.1, in AFDEX V24R01, all input data can be entered together in the pre-processor to offer greater convenience.

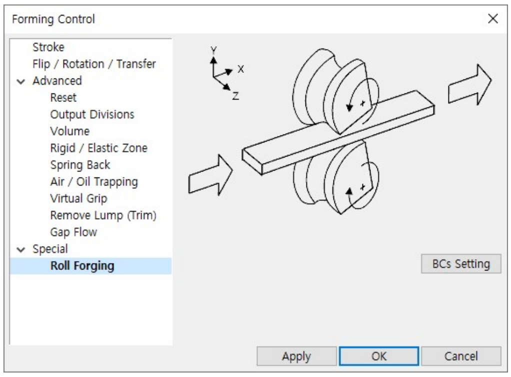

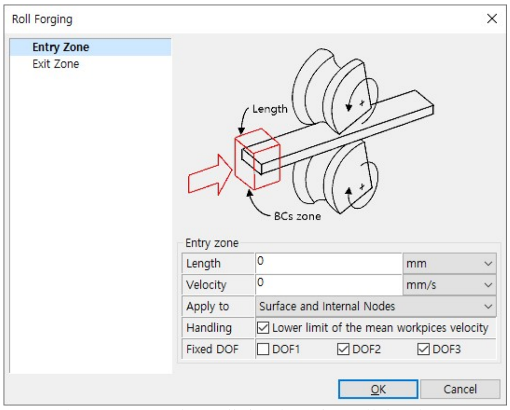

Figure 2.1 Settings dialog box for roll forging

2.2 Visualization of Contact Region between Models during Multi-body Analysis

Previously, in the multi-body analysis results, a contact region between CAD models could not be easily detected. AFDEX V24R01 provides the enhanced feature that display the contact region between all models, including die-workpiece as well as workpiece-workpiece. Figure 2.2 shows an example of applying the new function to the example in which three models are deformed by two dies and a binder. Users can visually check if there is any contact between different models with different colors. The two colors at the bottom (yellow, pink) represent the contact state between the three deforming bodies.

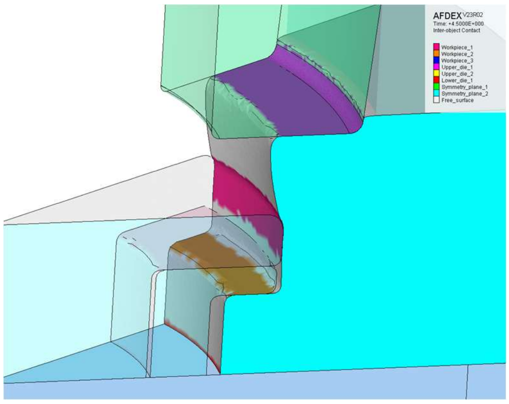

Figure 2.2 Contact area between objects

3. AFDEX_V24R01 Improvements

3.1 Feature Enhancement: Error Detection for 3D STL File

STL file format is widely used for 3D models of dies and workpieces in AFDEX metal forming simulation.

For an analysis model, it is possible to run normal simulation successfully only if there are no 'surface open' or 'non-manifold' errors. Previous version does not provide the feature which detects non-manifold errors, so that there were cases where unknown errors occurred during simulations.

Now, in AFDEX V24R01, one can check the non-manifold error in a 3D STL model with the error as shown in Figure3.1 (b). By contrast, Figure 3.1 (a) shows that there are no errors when importing the STL file with the non-manifold errors.

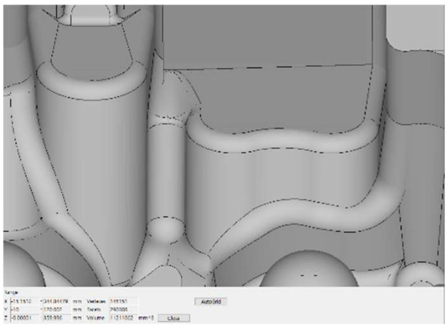

(a) Before improvement

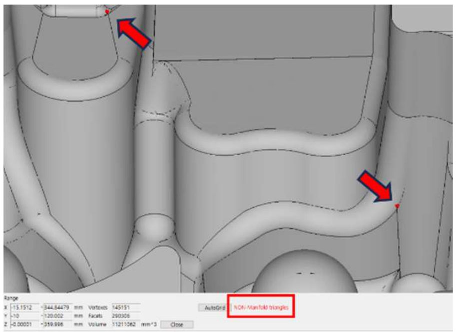

(b) After improvement

Figure 3.1 Error detection in 3D simulation

3.2 Overheating Prediction on Dies during Shape Drawing Process Simulation

In most metal forming processes that include forging, frictional heat is not an important factor, although friction itself is important. Therefore, most of the forging simulations do not pay attention to frictional heat. However, it becomes completely different situation in drawing process. In drawing process, a material generates relative motion such as slippage with dies, maintaining continuous contact with a certain part of a drawing die. In this case, lubrication for drawing and additives are widely used. However, there are limits of lubricants to solve the die overheating problems that can occur during the shape drawing, depending on the situation.

In AFDEX V24R01, users can control the frictional heat and predict the die overheating phenomenon (Prediction of friction heat ball) during the circular- and half-circular shape drawing process, using the feature that one can enter a temperature-dependent friction coefficient which is provided in AFDEX.

Figure 3.2 illustrates the overheating of a die caused by the frictional heat generated in narrow space, which occurred 5 seconds after the start of drawing. (Maximum temperature: 160℃) Considering the actual elapsed time of the process and a vicious cycle of frictional heat, temperature rise, and friction, the maximum temperature can increase significantly.

This overheated friction heat ball rapidly increases the surface temperature of the inflow of a workpiece, causing a rapid temperature softening of the flow stress at the surface of the workpiece. This can cause skin flow, and as shown in Figure 3.3, overlapping defects that are not understood by common sense can occur at the edges where are deformed. The phenomenon is more likely to occur in high-strength and high-temperature softening materials.

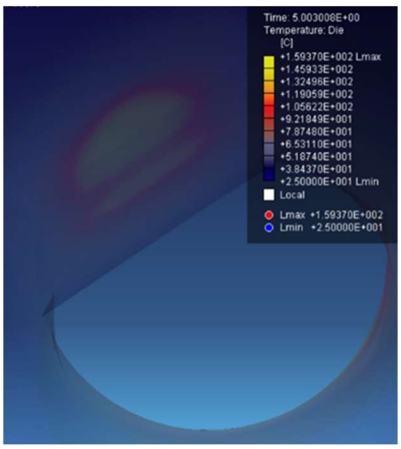

Figure 3.2 Overheating caused by friction at a drawing die

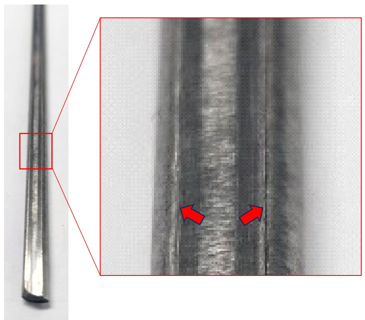

Figure 3.3 Folding occurred during circular- and half-circular shape drawing processes

4. Differentiated Features and the Latest Research using AFDEX

4.1 Shearing Simulation

Figure 4.1 shows a comparison between experiment and simulation for shearing process in automatic multi-stage cold forging process. For a short product which has a large influence by shearing such as a nut, the shape of the sheard material has a significant impact on the detailed stress distribution in vulnerable areas of a die. Therefore, the importance of shearing simulation is being highlighted to extend die life.

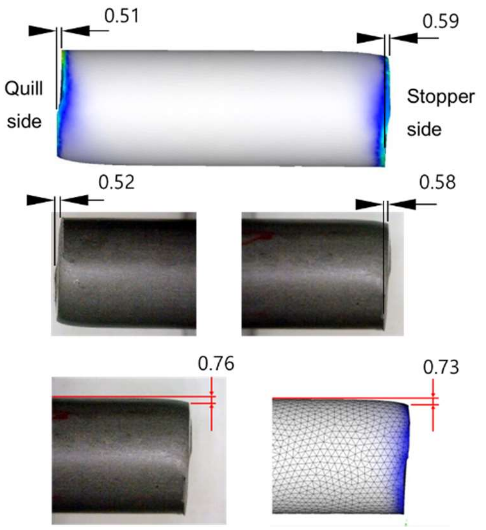

Figure 4.1 Comparison between experiment and simulation for shearing process [3]

Figure 4.2 shows the stress distribution on the die during automatic multi-stage cold forging for a nut, obtained using the initial shape of the sheared workpiece.

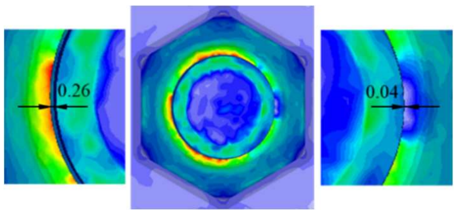

Figure 4.2 Effect of Sheared shape geometry on die stress

4.2 Coefficient of Friction depending on Temperature and Surface Strain

In metal forming simulation, the flow behavior of a material and friction influence prediction results. In case of forging simulation using a simple-shaped workpiece, an appropriate friction coefficient of a certain size predicts a reasonable result. However, the constant friction coefficient can predict simulation results that do not match the experimental results in some cases: cold forging process with unclear strain hardening (This increases the friction.), drawing process dependent on a lubricant (the temperature dependence is high.), extrusion or forging process for products with small thickness (frictional condition can affects a lot on the deformation locally).

AFDEX can easily consider the dependence of friction coefficient on temperature, pressure, strain, etc. Figure 3.2 is an example of an extreme dependence of the coefficient of friction on temperature in shape drawing process using a lubricant. Figure 4.3 (a) shows the simulation result of automatic multi-stage cold forging process for Aluminum steering yoke for passenger cars. It was able to predict the difference between left and right ear heights only in the case of the coefficient of friction is highly dependent on effective strain at the contact surface (The coefficient of friction rapidly increases when the effective strain of the material at the contact surface is around 1.6.), which the prediction shows a good agreement with the experimental results. This phenomenon has also been observed in hot forging of Aluminum alloys. [SW Lee, JM Lee, MS Joun, Tri. Int., 2020].

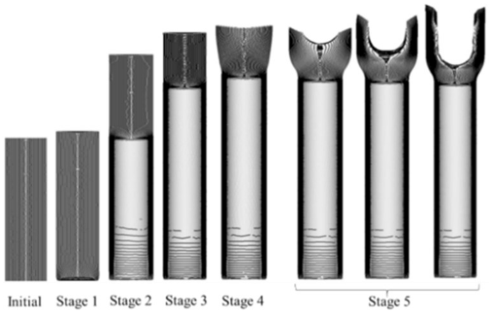

(a) Simulation results

(b) Experiment

Figure 4.3 Automatic multi-stage cold forging simulation of Aluminum steering yoke

4.3 Fillet Rolling (Burnishing) of Titanium Alloy Bolt for Aircraft Application

Imposing preload or compressive residual stress locally through burnishing greatly increases the resistance to fatigue failure of parts, that is, fatigue strength. Fillet rolling is a type of roller burnishing, which is a method of improving the local fatigue strength. Figure 4.4 shows the preload effective stress obtained by the fillet rolling process simulation with AFDEX.

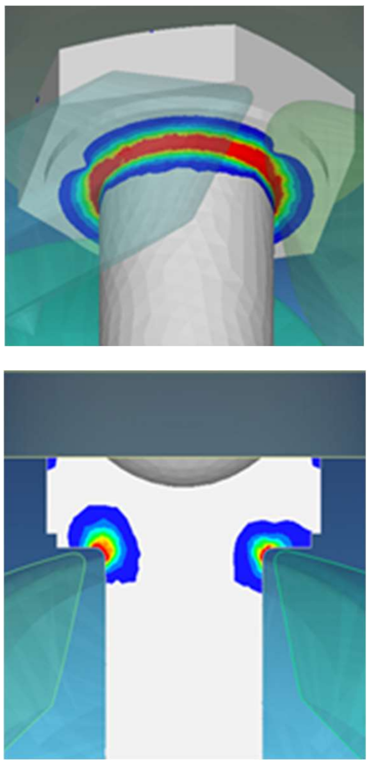

Figure 4.4 Effective stress in fillet rolling simulation

4.4 Application of Multi-body Analysis

Multi-body simulation is essential for solving a range of difficult metal forming process problems. In some cases, it needs to consider a die as an elastic body. In recent years an increasing number of applications of multi-body analysis have been introduced by developer groups.

Figure 4.2 shows the result of a die structural analysis with high precision, which is performed by multi-body analysis considering an ejector pin as an elastic body. Figure 4.5 and Figure 4.6 show the result of a simulation of construction rebar coupler testing and wire twisting process, respectively.

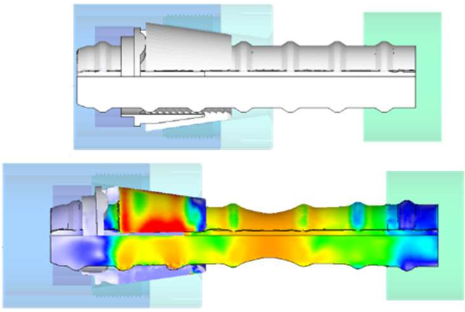

Figure 4.5 Simulation of construction rebar coupler testing

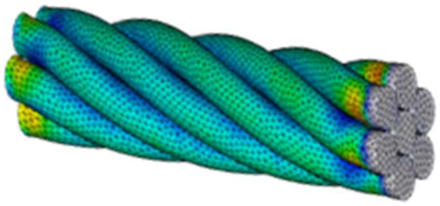

Figure 4.6 Simulation of wire twisting

4.5 Research Papers and Program Improvement

The following is the papers written by the developer groups over the past three years (2021-2023) which is the process of developing new functions and improving existing features of AFDEX. These papers providing a thorough overview of the theoretical basis and ideas of each possibility can inspire users to be of great help in developing into advanced users. Based on this, it will be an opportunity for developers and users to learn and develop each other. We would like to appreciate the AFDEX users and researchers for contributing to the writing of the following papers and hope to achieve greater progress.

<2021>

[1] M. S. Joun, H. J. Lee, S. G. Lim, K. H. Lee, G. S. Cho, 2021, Dynamic strain aging of an AISI 1025 steel coil and its relationship with macroscopic responses during the upsetting process, Int. J. Mech. Sci., V. 200, 106423.

[2] M. K. Razali, M. S. Joun, 2021, A new approach of predicting dynamic recrystallization using directly a flow stress model and its application to medium Mn steel, J. Mater. Res. Tech, V. 11, 1881-1894.

[3] M. S. Joun, S. W. Jeong, Y. T. Park, S. M. Hong, 2021, Experimental and numerical study on shearing of a rod to produce long billets for cold forging, J. Manuf. Process., V. 62, 797-805.

[4] M. K. Razali, M. S. Joun, W. J. Chung, 2021, A novel flow model of strain hardening and softening for use in tensile testing of a cylindrical specimen at room temperature, Materials, 14(17), 4876.

[5] D. W. Lee, R. Sekar, C. J. Lee, M. S. Joun, 2021, Influence of friction between materials on the axial direction pull force in single clinching, Trans. Mater. Process., V. 30, 83-90.

[6] H. N. Song, Y. S. Kim, M. S. Joun, 2021, The effects of theoretical models of materials and die on FE predictions in a forging process of aluminum scroll, Proc. Instit. Mech. Eng., Part E: J. Process Mech. Eng., V. 235(2), 274-284.

[7] M. K. Razali, S. W. Kim, M. Irani, M. C. Kim , M. S. Joun, 2021, Practical quantification of the effects of flow stress, friction, microstructural properties, and the tribological environment on macro- and micro-structure formation during hot forging, Tri. Int., V. 164, 107226.

[8] J. G. Eom, S. W. Byun, S. W. Jeong, W. J. Chung, M. S. Joun, 2021, A new methodology for predicting brittle fracture of plastically deformable materials: Application to a cold shell nosing process, Materials, V. 14(7), 1593.

[9] M. S. Joun, M. K. Razali, J. B. Byun, K. H. Lee, 2021, Accurate modelling of flow stress of AISI1025 at room temperature and its application to precision forging simulation, Forming the Future, The Minerals, Metals & Materials Series, 911-200.

[10] S. H. Chung, J. D. Yoo, M. S. Joun, 2021, Elastoplastic finite-element analysis of multi-body processes for joining mechanical parts, Forming the Future, The Minerals, Metals & Materials Series, 1451-1460.

[11] H. J. Lee, M. K. Razali, M. S. Joun, 2021, Flow stress characterization of carbon steel S25C in the temperature range of cold forming with an emphasis on dynamic strain aging, Mater. Today Commun., V. 28, 102483.

<2022>

[12] M. S. Joun, M. K. Razali, J. D. Yoo, M. C. Kim, J. M. Choi, 2022, Novel extended C-m models of flow stress for accurate mechanical and metallurgical calculations and comparison with traditional flow models, J. Magnes. Alloys, V. 10, pp. 2516-2533.

[13] M. S. Joun, S. M. Ji, J. D. Yoo, S. H. Chung, H. K. Moon, E. J. Kim, D. J. Yoon, J. M. Choi, A. Babu, 2022, Characterization of AZ31B, AZ61A and AZ80A magnesium alloys with an emphasis on temperature compensation for their application to a hot forging, J. Manuf. Proces., V. 84, pp. 764-785.

[14] M. S. Joun, J. B. Byun, W. J. Chung, K. H. Lee, 2022 A new general finite element method for predicting shearing and piercing, Int. J. Adv. Manuf. Technol. 120, 4581-4595.

[15] M. S. Joun, S. M. Ji, W. J. Chung, G. S. Cho, K. H. Lee, 2022, A new general fatigue limit diagram and its application of predicting die fatigue life during cold forging, Materials 15(7), 2351.

[16] M. S. Joun, M. K. Razali, C. W. Jee, J. B. byun, M. C. Kim, W, K. M. Kim, 2022, A review of flow characterization of metallic materials in the cold forming temperature range and its major issues, Materials 15(8), 2751.

[17] N. A. Razali, S. H. Chung, W. J. Chung, M. S. Joun, 2022, Implicit elastoplastic finite element analysis of tube-bending with an emphasis on springback prediction, Int. J. Adv. Manuf. Technol. 120, 6377-6391.

[18] S. M. Ji, S. M. Jang, Y. S. Lee, H. M. Kwak, J. M. Choi, M. S. Joun, 2022, Characterization of Ti-6Al-4V alloy in the temperature range of warm metal forming and fracture analysis of the warm capping process, J. Mater. Res. Technol., 18, 1590-1606.

[19] M. S. Joun, M. K. Razali, S. H. Chung, M. Irani, 2022, A direct method of calculating flow-related dynamic recrystallization parameters for generality and accuracy in predicting microstructural evolution, J. Mater. Res. Technol. 18, 3894-3907.

[20] J. B. Byun, C. W. Jee, I. D. Seo, M. S. Joun, 2022, Characterization of double strain-hardening behavior using a new flow parameter of extremum curvature strain of Voce strain-hardening model, J. Mech. Sci. Technol. V. 36, pp. 4115–4126.

[21] S. H. Chung, J. D. Yoo, H. K. Moon, W. J. Chung, M. S. Joun, 2022, Implicit elastoplastic finite element analysis of a wheel bearing shaft clinching process using the multi-body function, Metals, Vol. 12, 1930.

[22] K. M. Kim, J. B. Byun, J. H. Jeong, J. G. Kim, S. M. Hong, K. H. Lee, W. J. Chung and M. S. Joun, Fracture mechanism of AISI 1025 rod shearing in automatic multi-stage cold forging and critical shearing speed, Engineering Fracture Mechanics, 272 (2022) 108679.

[23] M. J. Cho, S. J. Kim, M. S. Joun, 2022, Optimal process design of an optimal, single-stage, symmetrical L-bending process employing taguchi method with finite element method, and experimental verification thereof, Int. J. Precis. Eng. Manuf. 23, 395-404.

[24] J. H. Park, S. M. Ji, J. M. Choi, M. S. Joun, Accurate flow characterization of A6082 for precision simulation of a hot metal forming process, Materials, V. 15, 8656.

<2023>

[25] S. H. Chung, S. W. Jeong, W. J. Chung, M .S. Joun, 2023, Realistic finite element analysis model of the pilgering process to deal with initial tube thickness nonuniformity, J. Manuf. Process., V. 95, pp. 217-228.

[26] S. M. Ji, J. M. Choi, M. S. Joun, 2023, Evaluation of the macroscopic formability of metallic materials using a cylinder compression test, J. Mater. Res. Technol., V. 23, pp. 2798-2809.

[27] K. M. Kim, S. M. Ji, S. W. Lee, S. M. Hong, M. S. Joun, 2023, Flow behavior dependence of rod shearing phenomena of various materials in automatic multi-stage cold forging. J. Mech. Sci. Technol., V. 37, 139–148.

[28] M. K. Razali, A. A. Ghawi, M. Irani, S. H. Chung, J. M. Choi, M. S. Joun, 2023, Practical approach for determining material parameters when predicting grain size after static recrystallization, J. Mater. Res. Technol., V. 23, pp. 3928-3941.

[29] J. B. Byun, C. W. Jee, K. H. Lee, M. S. Joun, 2023, General blending approach of fundamental cold flow models for an almost complete cold flow model in terms of tensile test, Steel Res. Int., V94., 2200540.

[30] M. K. Razali, A. A. Ghawi, M. Irani, S. H. Chung, J. M. Choi, M. S. Joun, 2023, Practical approach for determining material parameters when predicting austenite grain growth under isothermal heat treatment, Materials, V. 16, 6583.

[31] M. S. Joun, S. H. Chung, M. C. Lee, J. G. Eom, W. J. Chung, 2023, Cases of multi-body mechanics in metal forming, AIP Conf. Proc. 2571, 020003.

[32] R. Sekar, D. W. Lee, C. J. Lee, M. S. Joun, 2023, Finite element simulation of single point clinching process for its validation and process optimal design, AIP Conf. Proc. 2571, 020001.

[33] W. J. Chung, S. H. Chung, M. S. Joun, Three-dimensional elasto-thermoviscoplastic finite element method using tetrahedral MINI-element, AIP Conf. Proc. 2571, 020004.

5. Notice

5.1 Altair Partner Alliance Summit (APA)

From January 15-17, 2024, MFRC team took part in the Altair Partner Alliance Summit (APA) at Altair headquarter in Troy, Michigan for celebrating 15^{th} anniversary of the APA. The event provided a valuable opportunity for the APA partners to network with Altair team as well as other partners.

Figure 5.1 Altair and APA partners

5.2 AFDEX YouTube Channel

The tutorials and theories are uploaded on MFRC's YouTube channel. The following subjects will be provided: mathematical background, tensile testing, statics, solid mechanics, introduction to plasticity theory, finite strain, finite element method, and all materials related to metal forming, etc. Although the online lectures originally aim to help college students understand the materials, it can also be utilized as the materials introducing theories and mechanics used in AFDEX. For more details, please refer to the link below.
(https://www.youtube.com/c/AFDEX)